

# Observation of $J/\psi \rightarrow 3\gamma$

G. S. Adams,<sup>1</sup> M. Anderson,<sup>1</sup> J. P. Cummings,<sup>1</sup> I. Danko,<sup>1</sup> D. Hu,<sup>1</sup> B. Moziak,<sup>1</sup>  
 J. Napolitano,<sup>1</sup> Q. He,<sup>2</sup> J. Insler,<sup>2</sup> H. Muramatsu,<sup>2</sup> C. S. Park,<sup>2</sup> E. H. Thorndike,<sup>2</sup>  
 F. Yang,<sup>2</sup> M. Artuso,<sup>3</sup> S. Blusk,<sup>3</sup> S. Khalil,<sup>3</sup> J. Li,<sup>3</sup> R. Mountain,<sup>3</sup> S. Nisar,<sup>3</sup>  
 K. Randrianarivony,<sup>3</sup> N. Sultana,<sup>3</sup> T. Skwarnicki,<sup>3</sup> S. Stone,<sup>3</sup> J. C. Wang,<sup>3</sup> L. M. Zhang,<sup>3</sup>  
 G. Bonvicini,<sup>4</sup> D. Cinabro,<sup>4</sup> M. Dubrovin,<sup>4</sup> A. Lincoln,<sup>4</sup> P. Naik,<sup>5</sup> J. Rademacker,<sup>5</sup>  
 D. M. Asner,<sup>6</sup> K. W. Edwards,<sup>6</sup> J. Reed,<sup>6</sup> R. A. Briere,<sup>7</sup> T. Ferguson,<sup>7</sup> J. S. Y. Ma\*,<sup>7</sup>  
 G. Tatishvili,<sup>7</sup> H. Vogel,<sup>7</sup> M. E. Watkins,<sup>7</sup> J. L. Rosner,<sup>8</sup> J. P. Alexander,<sup>9</sup> D. G. Cassel,<sup>9</sup>  
 J. E. Duboscq,<sup>9</sup> R. Ehrlich,<sup>9</sup> L. Fields,<sup>9</sup> R. S. Galik,<sup>9</sup> L. Gibbons,<sup>9</sup> R. Gray,<sup>9</sup>  
 S. W. Gray,<sup>9</sup> D. L. Hartill,<sup>9</sup> B. K. Heltsley,<sup>9</sup> D. Hertz,<sup>9</sup> J. M. Hunt,<sup>9</sup> J. Kandaswamy,<sup>9</sup>  
 D. L. Kreinick,<sup>9</sup> V. E. Kuznetsov,<sup>9</sup> J. Ledoux,<sup>9</sup> H. Mahlke-Krüger,<sup>9</sup> D. Mohapatra,<sup>9</sup>  
 P. U. E. Onyisi,<sup>9</sup> J. R. Patterson,<sup>9</sup> D. Peterson,<sup>9</sup> D. Riley,<sup>9</sup> A. Ryd,<sup>9</sup> A. J. Sadoff,<sup>9</sup>  
 X. Shi,<sup>9</sup> S. Stroiney,<sup>9</sup> W. M. Sun,<sup>9</sup> T. Wilksen,<sup>9</sup> S. B. Athar,<sup>10</sup> R. Patel,<sup>10</sup> J. Yelton,<sup>10</sup>  
 P. Rubin,<sup>11</sup> B. I. Eisenstein,<sup>12</sup> I. Karliner,<sup>12</sup> S. Mehrabyan,<sup>12</sup> N. Lowrey,<sup>12</sup> M. Selen,<sup>12</sup>  
 E. J. White,<sup>12</sup> J. Wiss,<sup>12</sup> R. E. Mitchell,<sup>13</sup> M. R. Shepherd,<sup>13</sup> D. Besson,<sup>14</sup> T. K. Pedlar,<sup>15</sup>  
 D. Cronin-Hennessy,<sup>16</sup> K. Y. Gao,<sup>16</sup> J. Hietala,<sup>16</sup> Y. Kubota,<sup>16</sup> T. Klein,<sup>16</sup> B. W. Lang,<sup>16</sup>  
 R. Poling,<sup>16</sup> A. W. Scott,<sup>16</sup> P. Zweber,<sup>16</sup> S. Dobbs,<sup>17</sup> Z. Metreveli,<sup>17</sup> K. K. Seth,<sup>17</sup>  
 A. Tomaradze,<sup>17</sup> J. Libby,<sup>18</sup> A. Powell,<sup>18</sup> G. Wilkinson,<sup>18</sup> K. M. Ecklund,<sup>19</sup> W. Love,<sup>20</sup>  
 V. Savinov,<sup>20</sup> H. Mendez,<sup>21</sup> J. Y. Ge,<sup>22</sup> D. H. Miller,<sup>22</sup> I. P. J. Shipsey,<sup>22</sup> and B. Xin<sup>22</sup>

(CLEO Collaboration)

<sup>1</sup>*Rensselaer Polytechnic Institute, Troy, New York 12180, USA*

<sup>2</sup>*University of Rochester, Rochester, New York 14627, USA*

<sup>3</sup>*Syracuse University, Syracuse, New York 13244, USA*

<sup>4</sup>*Wayne State University, Detroit, Michigan 48202, USA*

<sup>5</sup>*University of Bristol, Bristol BS8 1TL, UK*

<sup>6</sup>*Carleton University, Ottawa, Ontario, Canada K1S 5B6*

<sup>7</sup>*Carnegie Mellon University, Pittsburgh, Pennsylvania 15213, USA*

<sup>8</sup>*Enrico Fermi Institute, University of Chicago, Chicago, Illinois 60637, USA*

<sup>9</sup>*Cornell University, Ithaca, New York 14853, USA*

<sup>10</sup>*University of Florida, Gainesville, Florida 32611, USA*

<sup>11</sup>*George Mason University, Fairfax, Virginia 22030, USA*

<sup>12</sup>*University of Illinois, Urbana-Champaign, Illinois 61801, USA*

<sup>13</sup>*Indiana University, Bloomington, Indiana 47405, USA*

<sup>14</sup>*University of Kansas, Lawrence, Kansas 66045, USA*

<sup>15</sup>*Luther College, Decorah, Iowa 52101, USA*

<sup>16</sup>*University of Minnesota, Minneapolis, Minnesota 55455, USA*

<sup>17</sup>*Northwestern University, Evanston, Illinois 60208, USA*

<sup>18</sup>*University of Oxford, Oxford OX1 3RH, UK*

<sup>19</sup>*State University of New York at Buffalo, Buffalo, New York 14260, USA*

<sup>20</sup>*University of Pittsburgh, Pittsburgh, Pennsylvania 15260, USA*

<sup>21</sup>*University of Puerto Rico, Mayaguez, Puerto Rico 00681*

---

\* present address: Department of Physics, University of Texas, Austin, Texas 78712, USA

<sup>22</sup>Purdue University, West Lafayette, Indiana 47907, USA

(Dated: June 3, 2008)

## Abstract

We report the first observation of the decay  $J/\psi \rightarrow 3\gamma$ . The signal has a statistical significance of  $6\sigma$  and corresponds to a branching fraction of  $\mathcal{B}(J/\psi \rightarrow 3\gamma) = (1.2 \pm 0.3 \pm 0.2) \times 10^{-5}$ , in which the errors are statistical and systematic, respectively. The measurement uses  $\psi(2S) \rightarrow \pi^+\pi^- J/\psi$  events acquired with the CLEO-c detector operating at the CESR  $e^+e^-$  collider.

PACS numbers: 13.20.Gd, 12.38.Qk

Ortho-positronium (oPs), the  ${}^3S_1$   $e^+e^-$  bound state, decays to  $3\gamma$  almost exclusively and has long been a fertile ground for precision QED tests [1]. The analog to oPs $\rightarrow 3\gamma$  for quantum chromodynamics (QCD), three-photon vector quarkonium decay, has not yet been observed. The rate of three-photon  $J/\psi$  decays acts as a probe of the strong interaction [2], most effectively when expressed in relation to  $J/\psi \rightarrow \gamma gg$ ,  $J/\psi \rightarrow 3g$ , or  $J/\psi \rightarrow \ell^+\ell^-$  due to similarities at the parton level. Hence, measurements of  $\mathcal{B}_{3\gamma}$ ,  $\mathcal{B}_{\gamma gg}$ ,  $\mathcal{B}_{3g}$ , and  $\mathcal{B}_{\ell\ell}$  relative to one another (where  $\mathcal{B}_X \equiv \mathcal{B}(J/\psi \rightarrow X)$ ) provide crucial experimental grounding for QCD predictions [2–4].

In this Letter we report the first observation of  $J/\psi \rightarrow 3\gamma$ . Rate measurements for other rare or forbidden all-photon decays,  $J/\psi \rightarrow \gamma\gamma$ ,  $4\gamma$ ,  $5\gamma$ , and  $\gamma\eta_c$  with  $\eta_c \rightarrow \gamma\gamma$ , are also described. Previous searches for  $\omega$  and  $J/\psi$  decay to  $3\gamma$  have yielded branching fraction upper limits of  $1.9 \times 10^{-4}$  and  $5.5 \times 10^{-5}$ , respectively [5]. As with oPs,  $C$ -parity symmetry suppresses vector quarkonia decays to an even number of photons, and two-photon decays are forbidden by Yang’s theorem [6]. Ref. [7] reports the limit  $\mathcal{B}_{\gamma\gamma} < 2.2 \times 10^{-5}$  at 90% confidence level (C.L.). Five-photon decays are suppressed by an additional factor of (at least)  $\sim \alpha^2$ ; *c.f.*,  $\mathcal{B}(\text{oPs} \rightarrow 5\gamma) \sim 2 \times 10^{-6}$  [8].

Ignoring QCD corrections altogether, Ref. [4] predicts  $\mathcal{B}_{3\gamma}/\mathcal{B}_{\ell\ell} \approx \alpha/14$ ,  $\mathcal{B}_{3\gamma}/\mathcal{B}_{\gamma gg} \approx (\alpha/\alpha_s)^2/3$  and  $\mathcal{B}_{3\gamma}/\mathcal{B}_{3g} \approx (\alpha/\alpha_s)^3$ . Using the precisely measured  $\mathcal{B}_{\ell\ell}$  [5] in the first prediction implies  $\mathcal{B}_{3\gamma} \approx 3 \times 10^{-5}$ . The latter two suffer the uncertainty of what value of  $\alpha_s$  to employ at the charmed quark mass scale [2]. Assuming  $\alpha_s(m_c^2)=0.3$  and inserting the result from a recent CLEO measurement [9] ( $\mathcal{B}_{\gamma gg} \approx 0.09$  and  $\mathcal{B}_{3g} \approx 0.66$ ) into the latter two predictions gives  $\mathcal{B}_{3\gamma} \approx (0.9\text{--}1.6) \times 10^{-5}$ . The first-order perturbative QCD corrections [4] to these estimates are large, so these predictions should only be considered as approximate.

Events were acquired at the CESR  $e^+e^-$  collider with the CLEO detector [10], mostly in the CLEO-c configuration (95%) with the balance from CLEO III. The dataset corresponds to  $27 \times 10^6$  produced  $\psi(2S)$  mesons and  $(9.59 \pm 0.07) \times 10^6$   $\psi(2S) \rightarrow \pi^+\pi^-J/\psi$  decays [11]. Event selection requires the tracking system to find exactly two oppositely charged particles, corresponding to the  $\pi^+\pi^-$  recoiling from the  $J/\psi$ , and that the calorimeter have at least 2, 3, 4, 5, and 3 photon showers for the  $J/\psi \rightarrow \gamma\gamma$ ,  $3\gamma$ ,  $4\gamma$ ,  $5\gamma$ , and  $\gamma\eta_c(\rightarrow \gamma\gamma)$  samples, respectively. Photon candidates must have energy exceeding 36 MeV and, with respect to any shower associated with one of the charged pions, either be located (*a*) more than 30 cm away, or (*b*) between 15 cm and 30 cm from it *and* have a photon-like lateral shower profile. We require that photon candidates not be located near the projection of either pion’s trajectory into the calorimeter nor be aligned with the initial momentum of either pion within 100 mrad.

A two-step kinematic fit first constrains the beam spot and the two charged pion candidates to a common vertex, and then the vertexed  $\pi^+\pi^-$  and the most energetic  $n$  photon candidates to the  $\psi(2S)$  mass [5] and initial three-momentum, including the effect of the  $\simeq 3$  mrad crossing angle between the  $e^+$  and  $e^-$  beams. Tight quality restrictions are applied to the vertex ( $\chi^2_{\text{v}}/\text{d.o.f.} < 3$ ) and four-momentum ( $\chi^2/\text{d.o.f.} < 3$ ) fits. The mass recoiling against the  $\pi^+\pi^-$  must lie inside a window around the  $J/\psi$  mass,  $M(\pi^+\pi^--\text{recoil}) = 3087\text{--}3107$  MeV. Non- $J/\psi$  backgrounds are estimated by keeping a separate tally of events with  $M(\pi^+\pi^--\text{recoil})$  inside 2980–3080 MeV or 3114–3214 MeV, ranges which together are ten times wider than the signal window.

Events with *any* of the photon pairs in the mass windows 0.10–0.16 GeV, 0.50–0.60 GeV, or 0.90–1.00 GeV are rejected to eliminate contributions from decays with  $\pi^0$ ’s,  $\eta$ ’s, or  $\eta'$ ’s, the dominant sources of photons in  $J/\psi$  decays. For the  $3\gamma$  selection only, we require all pho-

ton pair masses be less than 2.8 GeV to eliminate potential contamination from  $\eta_c \rightarrow \gamma\gamma$ . This requirement effectively restricts the smallest energy photon to have energy exceeding 200 MeV. For the  $4\gamma$  and  $5\gamma$  samples only, the smallest shower energy must be above 120 MeV, and all lateral shower profiles must be photon-like. This last restriction on shower shape avoids feed-up from  $J/\psi \rightarrow \gamma\eta(')$ ,  $\eta(') \rightarrow \gamma\gamma$  events with one or more photon conversions between the tracking chambers and the calorimeter: in such cases the two showers from the conversion  $e^+$  and  $e^-$  overlap one another, thereby distorting both of their lateral profiles. For the  $\gamma\eta_c$  channel only, we restrict the search region to large  $M(\gamma\gamma)_{lg}$  and small  $M(\gamma\gamma)_{sm}$ , which are, respectively, the largest and smallest of the three two-photon mass combinations in the event. The signal region is chosen this way so as to keep backgrounds small. Specifically, the signal box is defined, in units of GeV, by  $0.16 < M(\gamma\gamma)_{sm} < 0.48$ ,  $2.985 < M(\gamma\gamma)_{lg} + 0.0935M(\gamma\gamma)_{sm} < 3.040$ .

Signal and background decay modes are modeled with Monte Carlo (MC) samples that were generated using the EVTGEN event generator [12], fed through a GEANT-based [13] detector simulation, and then exposed to event selection criteria. For  $J/\psi \rightarrow n\gamma$  signal decays, final state photon momenta are distributed according to phase-space. For  $J/\psi \rightarrow 3\gamma$ , the lowest order matrix element for ortho-positronium [14] is used as an alternate; compared to phase space, it modestly magnifies the configurations that are two-body-like and those with three nearly-equal-energy photons (at the expense of topologies lying between these two extremes). For the process  $J/\psi \rightarrow \gamma\eta_c$ , an  $\eta_c$  mass and width of 2979.8 MeV and 27 MeV, respectively, are used (both are close to the PDG values [5]) to generate a Breit-Wigner  $\gamma\gamma$ -mass distribution; alternate widths from 23-36 MeV and different lineshapes [15] are explored as systematic variations.

Distributions in  $M(\gamma\gamma)_{sm}$  vs.  $M(\gamma\gamma)_{lg}$  and  $M(\pi^+\pi^- - \text{recoil})$  for the  $J/\psi \rightarrow 3\gamma$  and  $J/\psi \rightarrow \gamma\eta_c(\gamma\gamma)$  samples are shown for data, signal MC samples, and likely background decays in Figs. 1 and 2, respectively.

In all modes, non- $J/\psi$  backgrounds are small and are subtracted statistically using  $M(\pi^+\pi^- - \text{recoil})$  sidebands in the data. We determine the backgrounds from  $J/\psi$  decays with an exhaustive study of Monte Carlo samples. Decays with  $J/\psi \rightarrow \gamma f_J$  (where  $f_J$  signifies any of the many isoscalar mesons in the mass range from 600-2500 MeV), followed by  $f_J \rightarrow \gamma\gamma$  pose a negligible threat for any of the target modes because the product branching fractions are extremely small (e.g.,  $\simeq 2 \times 10^{-8}$  for  $J/\psi \rightarrow \gamma f_2(1270)$ ,  $f_2(1270) \rightarrow \gamma\gamma$ ). The predominant source of backgrounds to the  $3\gamma$  sample is the  $\gamma\pi^0\pi^0$  final state. This type of event can survive the selection by having both  $\pi^0$  decay axes nearly parallel to their lines of flight, such that one photon of each pair has very low energy in the laboratory frame, and is therefore nearly irrelevant to conservation of four-momentum. An analysis by BES [16] found that the largest sources of  $J/\psi \rightarrow \gamma\pi^0\pi^0$  are from  $J/\psi \rightarrow \gamma f_J$  decays, specifically through  $f_2(1270)$  and  $f_0(2050)$ , followed in importance by  $f_0(1710)$ ,  $f_0(1500)$ , and a number of much smaller contributions from nearby resonances. However, not all relevant product branching fractions for  $J/\psi \rightarrow \gamma f_J$ ,  $f_J \rightarrow \pi^0\pi^0$  have been measured, those that are measured have large uncertainties, and interference effects among overlapping  $f_J$  may not be small. A method to normalize  $\gamma\pi^0\pi^0$  other than using measured branching fractions is employed to reduce systematic uncertainty. The  $\chi^2/\text{d.o.f.}$  distribution for  $\gamma\pi^0\pi^0$  decays has a characteristic shape, *nearly independent of  $\pi^0\pi^0$  mass*, as shown in Fig. 3: the region  $\chi^2/\text{d.o.f.}=5-20$ , where almost no signal is present, is used to establish the level of  $J/\psi \rightarrow \gamma\pi^0\pi^0$ . Figure 4 shows the  $\chi^2/\text{d.o.f.}$  distribution from data, MC signal and MC background and the small contribution from non- $J/\psi$  decays obtained from the  $M(\pi^+\pi^- - \text{recoil})$  sidebands. The 142

data events with  $\chi^2/\text{d.o.f.}=5\text{-}20$  contain  $J/\psi \rightarrow 3\gamma$  signal (3.4 events), non- $J/\psi$  background (3.2), and, using known branching fractions,  $J/\psi \rightarrow \omega\eta$ ,  $\eta \rightarrow \gamma\gamma$  (1.7),  $J/\psi \rightarrow \gamma\eta$ ,  $\eta \rightarrow \gamma\gamma$  (1.2),  $J/\psi \rightarrow \gamma\eta$ ,  $\eta \rightarrow 3\pi^0$  (1.2),  $J/\psi \rightarrow \gamma\eta'$ ,  $\eta' \rightarrow \gamma\omega$ ,  $\omega \rightarrow \pi^0\gamma$  (0.6), and  $J/\psi \rightarrow \gamma\pi^0$  (0.2). The remainder (130.5 events) serves to normalize the  $\gamma\pi^0\pi^0$  background component, which has a relative 8% statistical uncertainty.

As a cross check on the  $3\gamma$  background normalization, we perform a maximum likelihood fit to data in the entire  $J/\psi \rightarrow 3\gamma$   $\chi^2/\text{d.o.f.}=0\text{-}30$  region with the combination of shapes from MC of  $\gamma\pi^0\pi^0$  and  $3\gamma$  signal with floating normalizations for each, and a fixed  $J/\psi$ -sidebands contribution from data, scaled by a factor of 0.1. Using this method with different sources of the  $\gamma\pi^0\pi^0$  taken one at a time as 100% of the background results in an average signal size of 23.3 events (with variation from 22.8 to 24.1), which is 0.9 events smaller than our nominal technique. Based on these numbers we assign a systematic error of 0.9 events, or  $\simeq 5\%$  relative, for signal extraction and background estimation for  $J/\psi \rightarrow 3\gamma$ .

The  $\chi^2/\text{d.o.f.}$  fit just described is repeated with the  $3\gamma$  signal shape weight fixed to zero. The likelihood difference with respect to the nominal fit provides a measure of the statistical significance of the signal. This significance varies from  $5.9\sigma$  to  $6.6\sigma$  when using any one of the backgrounds  $\gamma f_2(1270)$ ,  $\gamma f_0(1500)$ ,  $\gamma f_0(1710)$ ,  $\gamma f_0(2020)$ ,  $\gamma\pi^0\pi^0$  (phase space) as the sole contributor to the background shape.

MC studies indicate the following primary sources of backgrounds for the other modes: for the  $2\gamma$  sample,  $J/\psi \rightarrow \gamma\pi^0$  (3.3 events) and  $\gamma\eta$ ,  $\eta \rightarrow \gamma\gamma$  (2.7); for the  $4\gamma$  sample,  $J/\psi \rightarrow \gamma\eta$ ,  $\eta \rightarrow \gamma\gamma$  (0.9) or  $\eta \rightarrow 3\pi^0$  (0.8),  $\gamma\eta'$ ,  $\eta' \rightarrow \gamma\gamma$  (0.3) or  $\eta' \rightarrow \gamma\omega$ ,  $\omega \rightarrow \pi^0\gamma$  (0.9) or  $\eta' \rightarrow \pi^0\pi^0\eta$ ,  $\eta \rightarrow \gamma\gamma$  (0.3); for the  $5\gamma$  sample,  $J/\psi \rightarrow \gamma\eta$ ,  $\eta \rightarrow 3\pi^0$  (0.2) and  $\gamma\eta'$ ,  $\eta' \rightarrow \pi^0\pi^0\eta$ ,  $\eta \rightarrow \gamma\gamma$  (0.3); for  $\gamma\eta_c$ ,  $J/\psi \rightarrow \gamma\eta$ ,  $\eta \rightarrow \gamma\gamma$  (0.3),  $\gamma\eta'$ ,  $\eta' \rightarrow \gamma\gamma$  (0.2), and our newly found signal,  $J/\psi \rightarrow 3\gamma$  (0.3).

Numerical results appear in Table I. Net yield uncertainties and upper limits on event counts include the effects of statistical fluctuations in signal and background estimates. Signal efficiencies range from  $\simeq 2\%$  ( $5\gamma$ ) to  $\simeq 22\%$  ( $3\gamma$ ), and  $J/\psi \rightarrow 3\gamma$  is the only mode with a clear signal: 37 events observed on a background of 12.8. Statistics dominate the overall uncertainties for all decay modes. The  $J/\psi \rightarrow 3\gamma$  efficiencies for pure phase-space and the oPs matrix element are equal to within  $(0.2\pm 0.1)\%$ ; nevertheless, a 15% systematic error is assigned to allow for different behavior in the much heavier  $J/\psi$  system. For  $\gamma\eta_c$ , uncertainties in the lineshape, background, and  $\Gamma(\eta_c)$  dominate the systematic error.

Using the recently determined  $\mathcal{B}(J/\psi \rightarrow \gamma\eta_c) = (1.98 \pm 0.09 \pm 0.30)\%$  [15], the  $\eta_c \rightarrow \gamma\gamma$  branching fraction can be calculated as  $\mathcal{B}(\eta_c \rightarrow \gamma\gamma) = (0.6^{+1.3}_{-0.5} \pm 0.1) \times 10^{-4}$ , or  $< 3 \times 10^{-4}$  at 90% C.L. This value is consistent with the PDG [5] fit value of  $(2.7 \pm 0.9) \times 10^{-4}$  at the level of  $1.3\sigma$ , although making a meaningful comparison is difficult because the PDG number depends indirectly upon previous, considerably smaller values for  $\mathcal{B}(J/\psi \rightarrow \gamma\eta_c)$ .

In conclusion, we have investigated decays  $J/\psi \rightarrow n\gamma$  with  $n = 2, 3, 4, 5$ , where the photons are produced in direct decay, not through an intermediate resonance. For  $n=3$ , a signal of  $6\sigma$  significance is found with branching fraction  $\mathcal{B}_{3\gamma} = (1.2 \pm 0.3 \pm 0.2) \times 10^{-5}$ . This value lies between the zeroth order predictions [4] for  $\mathcal{B}_{3\gamma}/\mathcal{B}_{\gamma gg}$  and  $\mathcal{B}_{3\gamma}/\mathcal{B}_{3g}$  and is consistent with both, but is a factor of  $\simeq 2.5$  below that of  $\mathcal{B}_{3\gamma}/\mathcal{B}_{\ell\ell}$ . This measurement represents the first observation of a three-photon meson decay. No signal is seen for  $n=2, 4$ , or  $5$ , and upper limits are set on the branching fractions, each of which is the most precise or only measurement. We also measure  $\mathcal{B}(J/\psi \rightarrow \gamma\eta_c) \times \mathcal{B}(\eta_c \rightarrow \gamma\gamma) = (1.2^{+2.7}_{-1.1} \pm 0.3) \times 10^{-6}$  or an upper limit of  $< 6 \times 10^{-6}$  at 90% C.L., both consistent with other determinations [5].

We gratefully acknowledge the effort of the CESR staff in providing us with excellent

luminosity and running conditions. This work was supported by the A.P. Sloan Foundation, the National Science Foundation, the U.S. Department of Energy, the Natural Sciences and Engineering Research Council of Canada, and the U.K. Science and Technology Facilities Council.

---

- [1] S.G. Karshenboim, Int. J. Mod. Phys. A **19**, 3879 (2004); S. Asai *et al.*, arXiv:0805.4672v1 [hep-ex] (2008).
- [2] M.B. Voloshin, arXiv:0711.4556v3 [hep-ph] (2007), and Prog. Part. Nucl. Phys (in press).
- [3] A. Petrelli *et al.*, Nucl. Phys. **B514**, 245 (1998).
- [4] W. Kwong, P. B. Mackenzie, R. Rosenfeld and J. L. Rosner, Phys. Rev. D **37**, 3210 (1988).
- [5] W.-M. Yao *et al.* (Particle Data Group), J. Phys. **G33**, 1 (2006) and 2007 partial update for 2008.
- [6] C.N. Yang, Phys. Rev. **77**, 242 (1950); L. Landau, Phys. Abstracts **A52**, 125 (1949).
- [7] M. Ablikim *et al.* (BES Collab.), Phys. Rev. D **76**, 117101 (2007).
- [8] T. Matsumoto *et al.*, Phys. Rev. A **54**, 1947 (1996); Erratum A **56**, 1060 (1997).
- [9] D. Besson *et al.* (CLEO Collab.), arXiv:0806.0315v1 [hep-ex] (2008).
- [10] Y. Kubota *et al.* (CLEO Collab.), Nucl. Instrum. Meth. A **320**, 66 (1992); M. Artuso *et al.*, Nucl. Instrum. Meth. A **554**, 147 (2005); D. Peterson *et al.*, Nucl. Instrum. Meth. A **478**, 142 (2002); CLEO-c/CESR-c Taskforces & CLEO-c Collab., Cornell University LEPP Report No. CLNS 01/1742 (2001), unpublished.
- [11] H. Mendez *et al.* (CLEO Collab.), arXiv:0804.4432v1 [hep-ex] (2008). Accepted for publication in Phys. Rev. D.
- [12] D.J. Lange, Nucl. Instrum. Methods Phys. Res., Sect. A **462**, 152 (2001).
- [13] R. Brun *et al.*, Geant 3.21, CERN Program Library Long Writeup W5013 (1993), unpublished.
- [14] A. Ore and J.L. Powell, Phys. Rev. **75**, 1696 (1949); G.S. Adkins, arXiv:hep-ph/0506213v1 (2005).
- [15] R.E. Mitchell *et al.* (CLEO Collab.), arXiv:0805.0252v1 [hep-ex] (2008).
- [16] M. Ablikim *et al.* (BES Collab.), Phys. Lett. B **642**, 441 (2006).

TABLE I: Results for the five  $J/\psi \rightarrow n\gamma$  decay modes, showing the raw number of signal candidate events, estimated background levels, statistical significance of each signal, the net event yield and its 90% C.L. upper limit (UL), the signal efficiency, different sources of systematic error and their quadrature sum, expressed in percent of the central value ( $3\gamma$ ,  $\gamma\eta_c$ ) or of the UL (others), the branching fraction  $\mathcal{B}(J/\psi \rightarrow X)$  [first error is statistical, second is systematic], and the corresponding 90% C.L. upper limit UL, including effects of systematic errors.

	$2\gamma$	$3\gamma$	$4\gamma$	$5\gamma$	$\gamma\eta_c, \eta_c \rightarrow \gamma\gamma$
Signal candidates (events)	9	37	5	0	2
Background estimates (events)					
$J/\psi$ backgrounds	6.2	11.9	3.2	0.5	0.8
Non- $J/\psi$ backgrounds	0.9	0.9	0.5	0	0
Background sum (events)	7.1	12.8	3.7	0.5	0.8
Statistical significance ( $\sigma$ )	1.1	6.3	1.0	0.0	1.0
Net yield (68% C.L. interval) (events)	$1.9^{+4.7}_{-1.6}$	$24.2^{+7.2}_{-6.0}$	$1.3^{+2.4}_{-1.3}$	$0^{+1.2}_{-0}$	$1.2^{+2.8}_{-1.1}$
UL @ 90% C.L. (events)	$<7.7$	$<33.5$	$<6.0$	$<2.3$	$<4.7$
Efficiency (%)	19.2	21.8	8.71	1.90	10.9
Systematic uncertainties (%)					
Matrix element	0	15	15	15	15
$J/\psi$ background	15	5	10	0	15
$\pi^+\pi^- J/\psi$ counting	0.7	0.7	0.7	0.7	0.7
Detector modeling	4.5	6.4	8.3	10	6.4
$\Gamma(\eta_c)$	0	0	0	0	12
Quadrature sum (%)	16	17	20	18	25
$\mathcal{B}(J/\psi \rightarrow X) [10^{-6}]$		$12 \pm 3 \pm 2$			$1.2^{+2.7}_{-1.1} \pm 0.3$
UL on $\mathcal{B}(J/\psi \rightarrow X)$ @ 90% C.L. [ $10^{-6}$ ]	$<5$	$<19$	$<9$	$<15$	$<6$

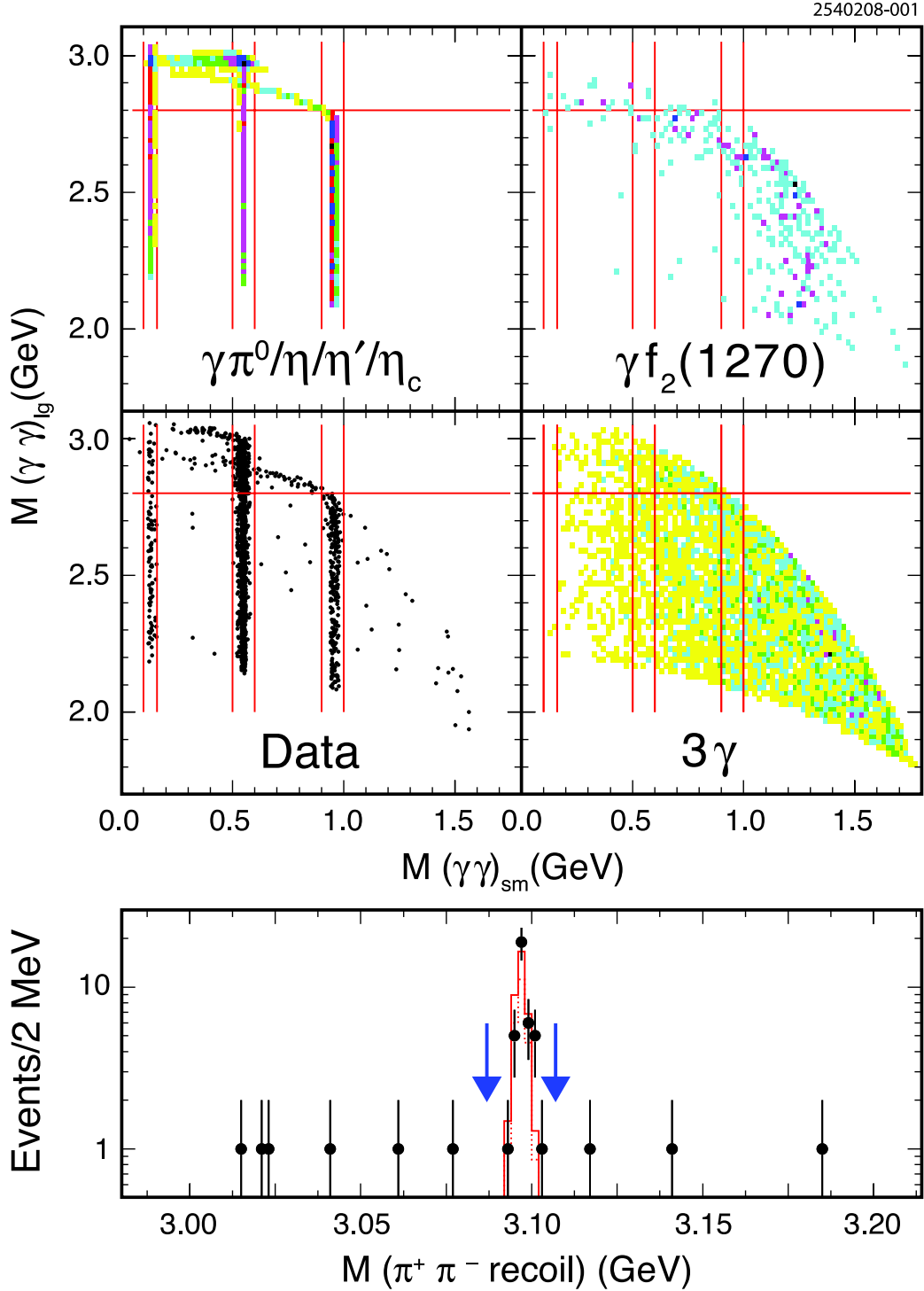


FIG. 1: Top four plots: in  $3\gamma$  data (lower left) and MC events for different  $J/\psi$  decays (top row and lower right), the largest vs. the smallest two photon mass combination per event. In the MC plots, darker shading of each bin signifies higher event density than lighter shading; in the data plot, each dot represents an event. The solid lines demarcate regions excluded from the  $J/\psi \rightarrow 3\gamma$  selection. Bottom plot: distribution of  $M(\pi^+ \pi^- \text{recoil})$  for the data events (points with error bars) overlaid with the  $J/\psi \rightarrow 3\gamma$  signal MC prediction (dotted line histogram) and MC background plus signal (solid line histogram) normalized to the data population. The arrows indicate the region of accepted recoil mass.

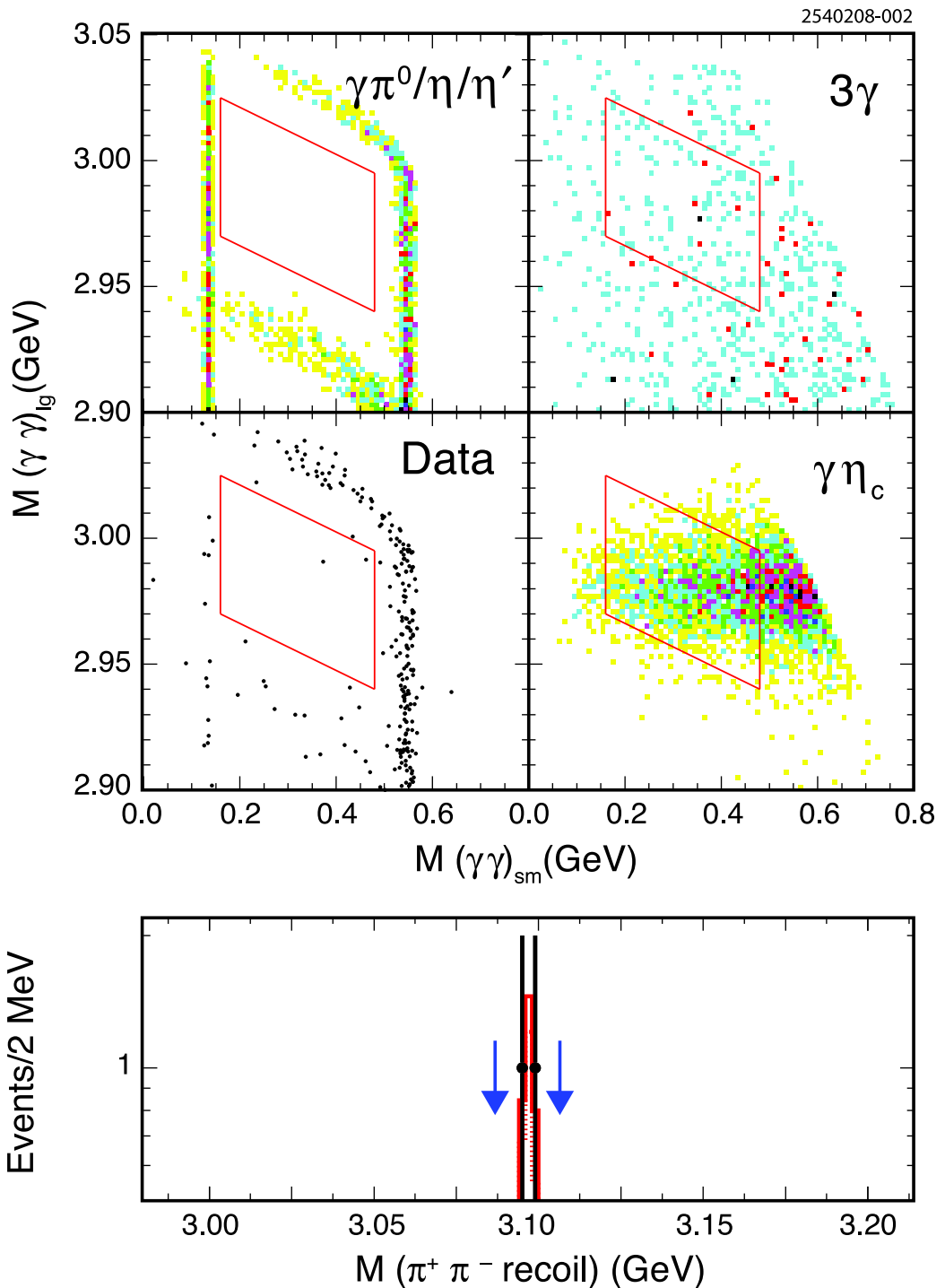


FIG. 2: As in Fig. 1, except zoomed in on the  $\eta_c$  region, and the overlaid parallelogram indicates the  $J/\psi \rightarrow \gamma\eta_c$  signal region. The  $M(\pi^+\pi^- \text{ recoil})$  distribution is for  $\gamma\eta_c$  candidates.

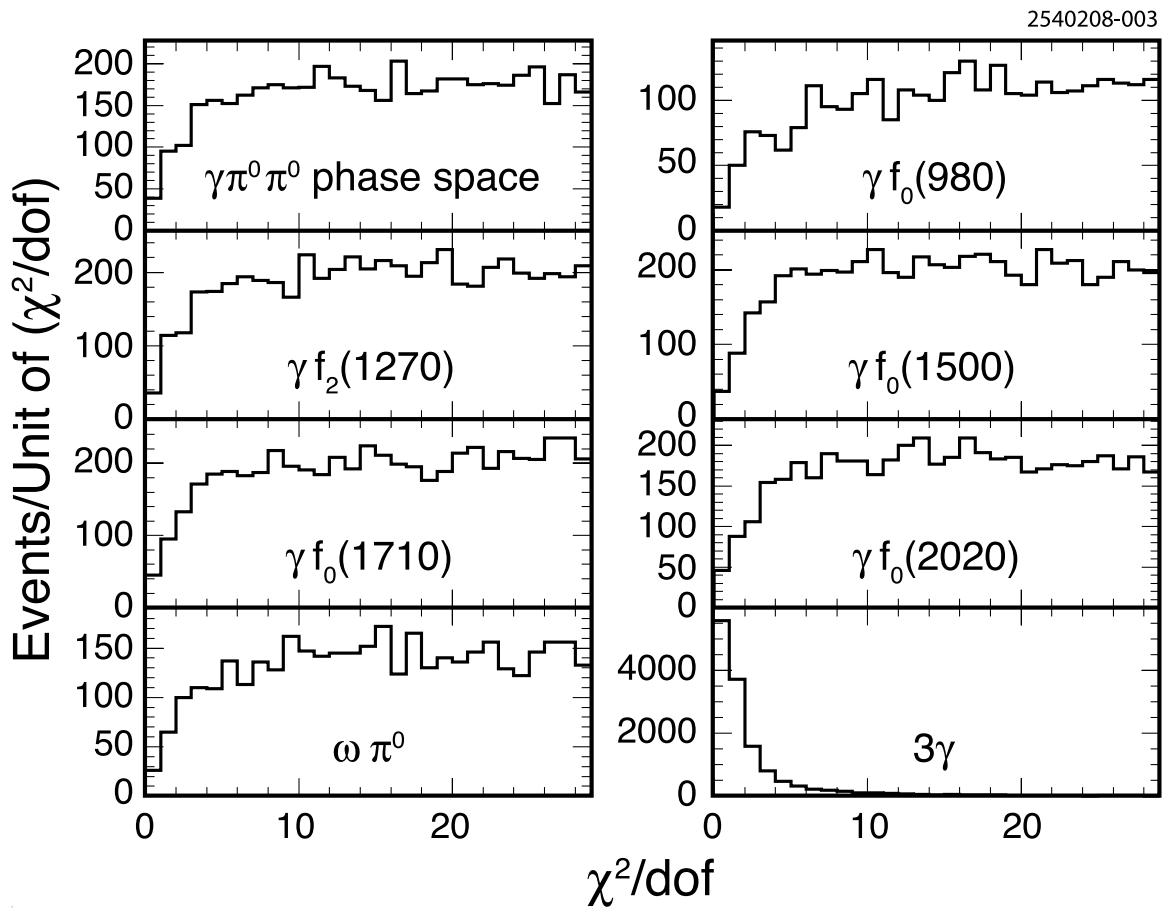


FIG. 3: The distribution of  $\chi^2/\text{d.o.f.}$  for  $J/\psi \rightarrow 3\gamma$  (lower right) and several sources of  $\gamma\pi^0\pi^0$  background.

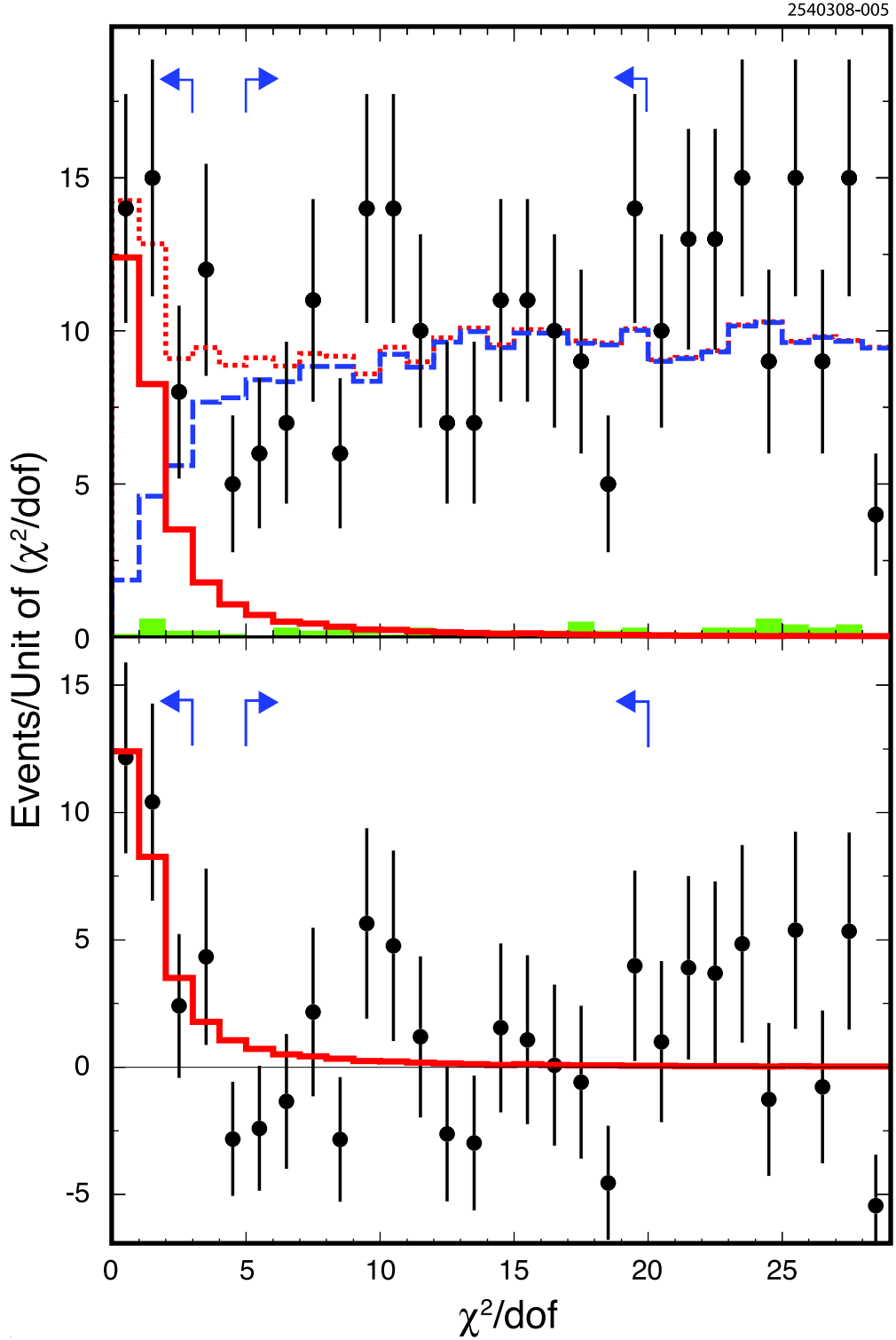


FIG. 4: The distribution of  $\chi^2/\text{d.o.f.}$  for  $J/\psi \rightarrow 3\gamma$ , in the top plot showing data (points with error bars) overlaid with the sum (dotted line histogram) of three components: non- $J/\psi$  background from scaled data sidebands (shaded histogram) and MC predictions for signal (solid) and  $J/\psi \rightarrow \gamma\pi^0\pi^0$  background (dashed). The bottom plot shows the same distribution, but with the MC and non- $J/\psi$  background subtracted from the data. The arrows indicate the values for signal selection and background normalization.